Digital Image Correlation, Acoustic Emission and Ultrasonic Pulse Velocity for the Detection of Cracks in the Concrete Buffer of the Belgian Nuclear Supercontainer

Sokratis ILIOPOULOS [a], Eleni TSANGOURI [a], Dimitrios G. AGGELIS [a], Lincy PYL [a], John VANTOMME [a, b], Philippe VAN MARCKE [c], Lou AREIAS [d, a]

[a] Department of Mechanics of Materials and Constructions, Vrije Universiteit Brussel, Pleinlaan 2, 1050 Brussels, Belgium
[b] Civil and Material Engineering Department, Royal Military Academy, Renaissancelaan 30, 1000 Brussels
[c] ONDRAF/NIRAS, Belgium
[d] EURIDICE GIE/SCK•CEN Mol, Belgium

Abstract. The long term management of high-level and heat emitting radioactive waste is a worldwide concern, as it directly influences the environment and future generations. To address this issue, the Belgian Agency for Radioactive Waste and Enriched Fissile Materials has come up with the conceptual design of a massive concrete structure called Supercontainer. The feasibility to construct these structures is being evaluated through a number of scaled models that are tested using classical as well as state of the art measurement techniques. In the current paper, the results obtained from the simultaneous application of the Digital Image Correlation (DIC), the Acoustic Emission (AE) and the Ultrasonic Pulse Velocity (UPV) nondestructive testing techniques on the second scaled model for the detection and monitoring of cracks will be presented.

1. Introduction

The reference solution for the long term management of high-level and heat emitting radioactive waste is considered by ONDRAF/NIRAS (the Belgian Agency for Radioactive Waste and Enriched Fissile Materials) to be the geological disposal in poorly indurated clay [1,2]. Before their transportation to an underground repository, the high level wastes (HLW) are post-conditioned in so called supercontainers. The supercontainers are cylindrical structures which consist of four engineering barriers that from the inner to the outer surface are namely: the overpack, the filler, the concrete buffer and the envelope. The overpack, which is made of carbon steel, is the place where the vitrified wastes and spent fuel are stored. The buffer, which is made of concrete, creates a highly alkaline environment ensuring slow and uniform overpack corrosion as well as radiological

shielding. In-between the two materials the cementitious filler exists with slightly different material properties compared to the concrete buffer.

In order to evaluate the feasibility to construct such supercontainers two scaled models have so far been designed and tested by SCK/CEN (the Belgian Nuclear Research Centre). These cylindrical models have the diameter of a real supercontainer (2.11 m) but a height approximately half of the real dimension (3.45 m), as shown in figure 1a [3,4,5]. The supercontainer concept comprises four construction phases that are simulated in the same way by the scaled models. The only difference is that instead of the high level and heat emitting waste, an electrical heat source delivering a constant power of 300 W/m is used. Concerning the other construction phases of the supercontainer and the scaled models, first the outer concrete buffer is cast and then the hot overpack (containing either waste canisters or heat elements), the filler and the lid are installed successively. The first construction phase is called the ''cold phase'' whereas construction phases two to four define the ''heating phase''.

The first scaled model that was performed to evaluate the feasibility to construct the supercontainer indicated crack formation on the surface of the concrete buffer. The absence of a crack detection and monitoring system precluded defining the exact time of crack initiation, as well as their origin, the penetration depth, the crack path and the propagation history. For this reason, the second scaled model test was performed to obtain further insight by answering to the aforementioned questions. In this model, reliable and inexpensive non-destructive testing techniques were incorporated. The present paper comprises the results of three state of the art techniques; the Digital Image Correlation (DIC), the Acoustic Emission (AE) and the Ultrasonics Pulse Velocity (UPV) which were specifically adapted for this second test in order to detect and monitor the surface and through the depth fracture behaviour [6-11].

2. Experimental Details

In order to construct the second scaled model of the supercontainer a carbon steel ASTM A 106 Gr B mould was used, as shown in figure 1b. This mould consisted of two half-cylindrical parts that were fastened together by means of bolts in order to create the final shell. The mould had a thickness of 5 mm. One of the two metal parts contained three rectangular windows of 430 mm in width and 530 mm in height at three different levels across the height of the scaled model (figure 1b). These windows were designed beforehand in order to give access to measurements with the DIC technique as early as possible (just 2 days after casting of the concrete buffer). A steel frame was welded to the bottom steel platform of the mould shown in figure 1b. This steel frame was designed to support the square stereo bar holding the two CCD cameras. The frame had a distance of approximately 700 mm from the concrete buffer outer surface. Two CCD (Charge Coupled Devices) cameras from LIMESS were used for the specific application with a resolution of 1628 x 1236 pixels. The Q-400 Digital 3D Image Correlation system from DANTEC GmbH was used for the second scaled model. A pair of 12 mm lenses was used in order to achieve the experimental resolution of 3-4 pixels/mm. Three arbitrary speckle patterns were painted with the aid of a silica screen onto the surface of the second scaled model at three different levels. The result is shown in figures 2a,b. The cameras system was calibrated using a dedicated calibration plate (35 mm) from DANTEC GmbH. The analysis of the digital images was performed with the ISTRA 4D software of the same company.

The AE and UPV setup included the use of resonant acoustic emission sensors (R15) with resonance frequency 150 kHz, amplifiers, a computer with four channels and embedded software for the analysis of the emitted signals. The first scaled model test

showed that the maximum temperature in the outer surface occurred approximately on the level of the second DIC window. For this reason, it was decided the sensors to surround the middle DIC window in a rectangular configuration. The sensors were either applied to the outer mould of the concrete buffer until its removal (see figure 2a) or directly to the concrete surface for the remaining period of the test (see figure 2b). The removal of the outer mould was conducted 29 days after casting of the concrete buffer. The casting of the buffer signified the beginning of the test and the beginning of the first phase. In the first case (sensors attached to the mould) the horizontal distance between the sensors was 500 mm whereas the vertical distance was 300 mm. In the second case (sensors attached to the concrete buffer) the horizontal and vertical distance of the sensors was 370 mm and 300 mm respectively. In both cases a velocity test was performed. The velocity test can provide the velocity of the pulse travelling through the examined concrete buffer. Knowing the velocity it is easy to extract the location of the active sources from the different transient times recorded from each sensor. The amplitude of the detected signals is amplified with the aid of the amplifiers. The signals are then digitized, stored and analyzed with the computer embedded software. The AE measurement system used in the second scaled model was the micro-SAMOS system from MISTRAS Holdings.

(a)

(b)
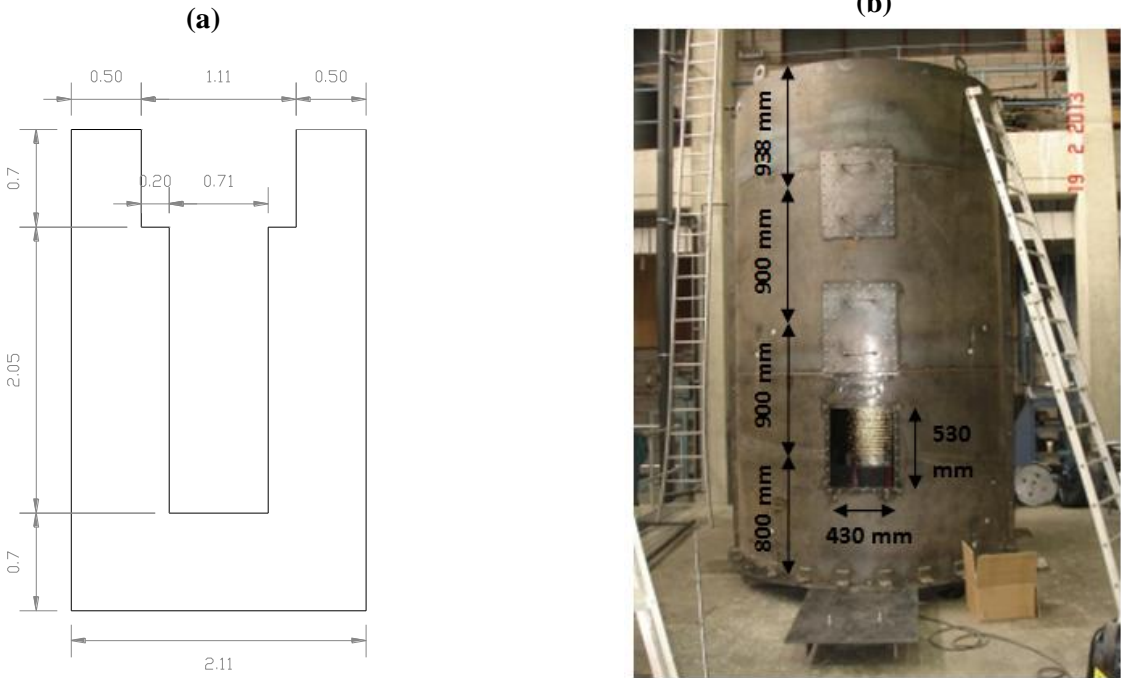
Figure 1 (a) Simplified cross-section of the second scaled model showing the concrete buffer of the outer surface [dimensions in m] and **(b)** assembled mould where one part contains 3 windows needed for the application of the DIC technique
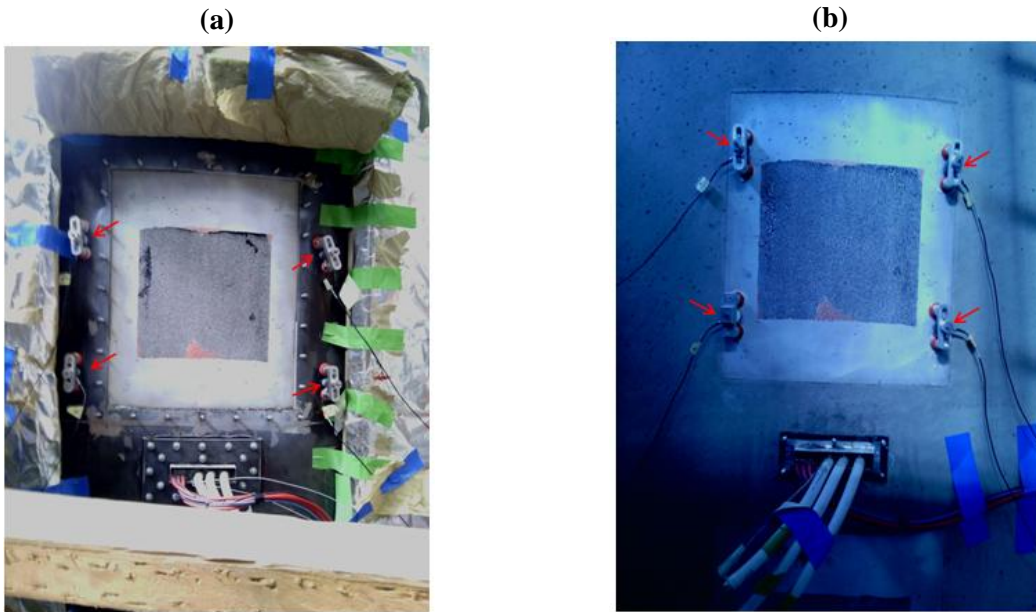
Figure 2 The speckle pattern of Window 2 (middle window) and 4 acoustic emission sensors (red arrows) **(a)** attached to the mould until its removal (phase 1), **(b)** mounted on the concrete surface after the removal (day 29)

3. Results

The DIC/AE/UPV results that will be presented in this paper focus only on the ''heating phase'' (or phase 2), after the installation of the heater, where the exact time, the location and the width and depth of cracks were determined.

3.1 Exact time and location of crack initiation

The casting of the filler (second phase concrete) occurred 56 days after casting of the concrete buffer (first phase concrete) on 11/06/2013. This action signified the beginning of phase 2 (time zero of phase 2 = 56 days of phase 1). One day earlier, the hot overpack containing heating elements was installed in the cavity created from the casting of the first phase concrete. As shown from figure 3a, till the end of phase 1 (11 June) no crack initiation was observed across the height of the scaled model. On the other hand, a few days later cracking was visualized by means of the DIC technique. During this week, AE was continuously monitoring the behavior of the scaled model, whereas several and frequent measurements were conducted by the DIC technique. Figure 3a, depicts the different dates of phase 2 that cracking was observed for each window of the scaled model. Crack initiated first at the middle window (W2) and then at the top and bottom window successively. It needs to be mentioned that DIC was not used for continuous monitoring. Therefore, cracking has occurred in a time between the capturing of the subsequent images. If we focus on the middle window where cracking was firstly detected we can figure out the exact time of crack initiation by means of AE technique. In figure 3b the cumulative AE events are plotted as a function of time during the first days of phase 2. In this figure, a rapid increase (almost vertical line) of the AE events is seen after approximately 16.7 hours of continuous AE monitoring. This means that less than 2 days after the insertion of the hot overpack (08.40 AM) there is an indication of crack initiation. This AE indication was confirmed the same day a few hours later (11.30 AM) by the DIC technique (figure 3c). Except from the identification of the exact time of crack initiation by the AE technique and

the proof by the DIC technique, the AE location output is compatible with the visual output of the DIC technique especially near AE sensor 3 on the bottom right corner of the DIC window. A concentration of AE sources above and to the right of sensor 4 (location approximately [X=100mm, Y=150mm]) is also close to the path of the other diagonal crack at the bottom left of the DIC strain field. This convergence between the two techniques makes it clear that the combination of them can neutralize the weaknesses of each technique and validate the results individually obtained.
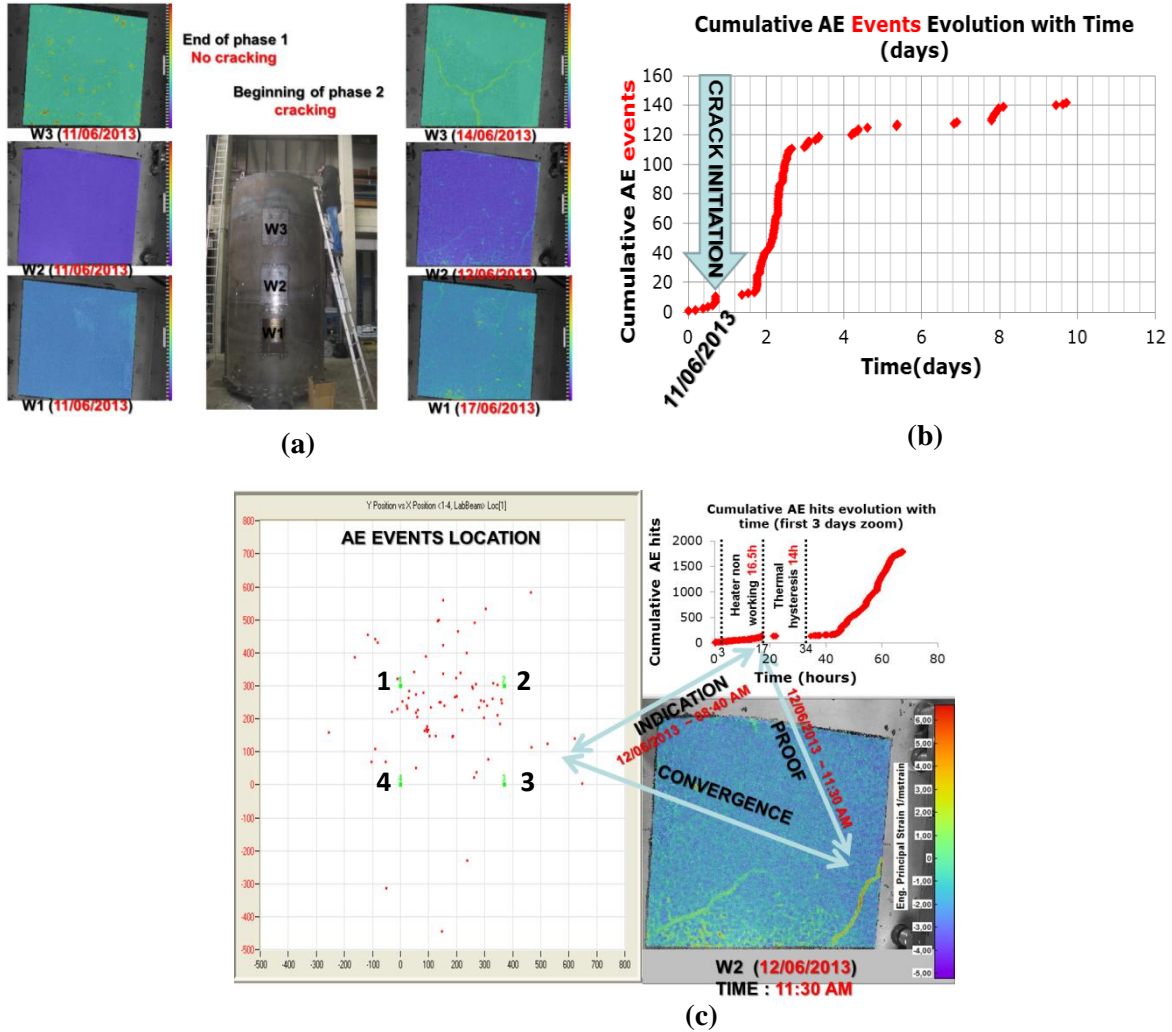
Figure 3 **(a)** No crack initiation before the insertion of the hot overpack (left images) compared to the beginning of phase 2 (right images) in terms of the first principal engineering strain **(b)** Cumulative AE activity vs time showing crack initiation approximately 20 hours after casting of filler (08:40 AM) and **(c)** confirmation the same day a few hours later (11:30 AM) on the same height level by DIC technique.

3.2 Width of the cracks

Post processing analysis of the captured digital images at the three different levels across the height of the structure provided not only the width of the cracks at the time of crack initiation but also the evolution of the crack width through the days of the second phase of the test. The results indicated an increasing tendency of the crack width for all windows with initial values equal to 15±5 micrometers for Window 1 (17/06/2013), 20±5 micrometers for Window 2 (12/06/2013) and 30±10 micrometers for Window 3 (14/06/2013) corresponding to the day of crack initiation and peak values up to 60 micrometers for Window 1, up to 55 micrometers for window 2 and up to 140 micrometers

for window 3. It needs to be mentioned that the ± is used in order to take into account the different values of crack width taken the same day at different points across the crack.

3.3 Depth of cracks

One of the objectives of the second scaled model was to investigate the depth of the developed cracks. In order to measure crack depth the Ultrasonic Pulse Velocity (UPV) testing technique was performed in the laboratory of Mechanics of Materials and Constructions (MeMC) of the Vrije Universiteit Brussel (VUB). The reason for utilizing the UPV technique was that the DIC technique and the AE configuration of the sensors were such that they could only provide information on the surface and not on the 3rd dimension. A core sample drilled from the second scaled model of the supercontainer was tested by UPV. This cylindrical core sample had a length of 76.8 cm and a diameter of 14 cm. Two piezoelectric sensors were mounted on two opposite sides across the diameter of the specimen forming either a horizontal plane ''parallel'' to the crack or a vertical plane "perpendicular" to the crack. A generator creating the predefined pulse and a computer with suitable acquisition board for the digitization, storage and analysis of the waveforms were also needed. The result of the technique is depicted on figure 4. The blue dots describe the value of concrete pulse velocity perpendicular to the crack whereas the red dots are describing the measurements on the horizontal plane. Measurements were conducted at intervals of 10 mm along the axis of the cylinder. Each cm was ''scanned'' providing a clear view of the distance where the stabilization of the concrete pulse velocity had occurred. As shown in figure 4, the pulse velocity of the concrete obtains a constant high value at 38 cm concerning the vertical plane measurements indicating also the depth of crack. In order to confirm this finding, X-rays were applied on the same core sample. The X-rays results showed a diagonal crack that was running 38 cm through the depth as well. It needs to be mentioned that both UPV and X-rays are non-destructive techniques capable of quantifying the depth of a defect but the latter is expensive and bears danger to the operator and/or public health. Concerning the horizontal measurements UPV stabilizes in much shallower depth, due to the diagonal orientation of the crack that did not interact with the ultrasonic wave path parallel to it. From the same figure, a drop in concrete pulse velocity is shown at 70 cm followed by stabilization for the last 6 cm of the core length. The reason is the transition between the concrete buffer and the filler that takes place exactly at this position (the thickness of the concrete buffer is 70 cm). It is important to note that the filler has different material properties than the concrete buffer and is designed to have lower stiffness.
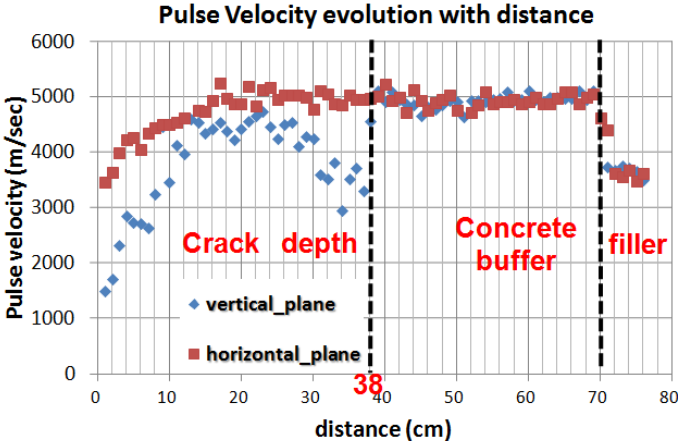
Figure 4 Measurement of the depth of a specific crack of the 2nd scaled model and identification of the interface between concrete buffer and filler by means of UPV technique

6

Complementary UPV measurements were also applied in situ on the scaled model at specific locations where indications of cracks existed.

4. Conclusions

The feasibility to construct the Supercontainer for the long term management of high level and heat emitting radioactive waste was evaluated through the test of a second scaled model. This scaled model included the use of reliable and inexpensive nondestructive techniques. These techniques were namely the Digital Image Correlation (DIC), the Acoustic Emission (AE) and the Ultrasonic Pulse Velocity (UPV). The AE technique indicated that 20 hours after casting of the filler and less than 2 days after the insertion of the hot overpack (phase 2) cracking initiated first at the middle DIC window (window 2) which was proved a few hours later from DIC measurements on the same level. It was also shown that cracking in the top window initiated 1 to 3 days after casting whereas cracking on the bottom window initiated 3 to 6 days after casting. The width of the cracks at the time of crack initiation was 15±5 micrometers for Window 1 (17/06/2013), 20±5 micrometers for Window 2 (12/06/2013) and 30±10 micrometers for Window 3 (14/06/2013) whereas the depth of a specific crack was equal to 38 cm by UPV and X-rays. In situ ultrasonic measurements on the depth of an imperfection presented time independent almost zero values except from a hole on the bottom of the imperfection which measured approximately 2.4 cm.

References

[1] ONDRAF/NIRAS, (2010), "Feasibility strategy and Feasibility Assessment Methodology for the geological disposal of radioactive waste," ONDRAF/NIRAS report NIROND-TR 2010-19 E

[2] ONDRAF/NIRAS,(2009), "The Long-Term Safety Strategy for the Geological Disposal of Radioactive Waste," ONDRAF/NIRAS report NIROND-TR 2009-14 E.

[3] Areias, L., I. Troullinous, S. Iliopoulos, E. Voet, L. Pyl, Ch. Lefevre, J. Verstricht, Y.Van Ingelgem, E. Coppens and Ph. Van Marcke (2013). Instrumentation and monitoring aspects of a ½-scale test to evaluate the feasibility of the Belgian Supercontainer, 15th ASME International Conference on Environmental Remediation and Radioactive Waste Management.

[4] Areias, L., Craeye, B., De Schutter, G., Van Humbeeck, H., Wacquier, W., Villers, L., Van Cotthem, A. (2010a). Half-scale test: an important step to demonstrate the feasibility of the Belgian Superconatiner concept for disposal of HLW. Proceedings 13th International Conference on Environmental Remediation and Radioactive Waste Management, ICEM2010, Tsukuba, Japan

[5] ESV EURIDICE GIE, ONDRAF/NIRAS (2011), First half-scale test, Construction and Test Results, Final Report, May 2011

[6] Aggelis D.G., Verbruggen S., Tsangouri E., Tysmans T., Van Hemelrijck D. (2013) Characterization of mechanical performance of concrete beams with external reinforcement by acoustic emission and digital image correlation, Construction and Building Materials 47 , 1037–1045

[7] Aggelis D.G., D.V. Soulioti, N. Sapouridis, N.M. Barkoula, A.S. Paipetis, T.E. Matikas (2011) Acoustic emission characterization of the fracture process in fibre reinforced concrete, Constructions and Building Materials 25 ,pp. 4126-4131

[8] Aggelis DG, Shiotani T, Momoki S, Hirama A. (2009) Acoustic emission and ultrasound for damage characterization of concrete elements. ACI Mater J;106(6):509–14.

[9] Grosse, C. U.; Ohtsu, M. (2008) Acoustic Emission Testing, Springer, Heidelberg, 2008

[10] Naik R.T, Malhotra V.M., Popovic S.J. (2004), The Ultrasonic Pulse Velocity Method, Chapter 8 of the book CRC Handbook on Nondestructive Testing of Concrete, Editor : N. Carino, by CRC Press LLC

[11] Sutton MA, Orteu JJ, Schreier HW.(2009) Image correlation for shape, motion and deformation measurements. Basic concepts, theory and applications. New York, USA: Springer Science + Business Media